ELSEVIER

Earth and Planetary Science Letters 165 (1999) 229–239

EPSL

Low-temperature properties of a single crystal of magnetite oriented along principal magnetic axes

Özden Özdemir *, David J. Dunlop

Department of Physics, University of Toronto at Mississauga, Mississauga, Ontario L5L 1C6, Canada

Received 3 September 1998; revised version received 23 November 1998; accepted 24 November 1998

Abstract

We have measured saturation induced and remanent magnetizations and induced magnetization as a function of field at low temperatures, between 300 K and 10 K, on an oriented 1.5-mm single crystal of magnetite. The induced magnetization curves along the cubic [001], [1$\bar{1}$0], and [110] axes at 10 K have very different approaches to saturation. The crystal is easy to magnetize along [001] but difficult along [1$\bar{1}$0] and [110], the hard directions of magnetization for monoclinic magnetite. The temperature dependence of saturation magnetization between the Verwey transition temperature, $T_v = 119$ K, and 10 K is also different along the three axes, indicating that below T_v the crystal has uniaxial symmetry. The room-temperature saturation remanence (SIRM) produced along [001] decreases continuously in the course of zero-field cooling, levelling out at the isotropic temperature, $T_i = 130$ K, where the first magnetocrystalline anisotropy constant becomes zero. At T_i, 86% of the initial SIRM was demagnetized. The domain wall pinning responsible for this soft remanence fraction must be magnetocrystalline controlled. The remaining 14% of the SIRM is temperature independent between T_i and T_v and must be magnetoelastically pinned. This surviving hard remanence is the core of the stable magnetic memory. The Verwey transition at 119 K, where the crystal structure changes from cubic to monoclinic, is marked by a discontinuous increase in remanence, indicating that the cubic [001] direction suddenly becomes an easy direction of magnetization. The formation of monoclinic twins may also affect the intensity of remanence below T_v. Reheating from 10 K retraces the cooling curve, with a decrease at T_v back to the original remanence level, which is maintained to 300 K. When SIRM is not along [001], the initial SIRM is larger but the reversible changes across the Verwey transition are much smaller. The SIRM produced at 20 K is an order of magnitude larger than the 300 K SIRM, but the only change during warming is a discontinuous and irreversible drop to zero at T_v.

Keywords: magnetite; Verwey transition; oriented transition; saturation isothermal remanence; monoclinic magnetite

1. Introduction

Magnetite (Fe_3O_4) has two magnetic transitions below room temperature. At the isotropic point T_i around 130 K, the first magnetocrystalline anisotropy constant (K_1) passes through zero, causing domain walls to unpin. At the Verwey transition, a crystallographic phase transition variously reported to occur at $T_v = 110$–125 K, the structure changes from cubic to monoclinic. In most previous studies, it has been difficult to separate with certainty the magnetic effects of the two transitions. For example, in the technique of low-temperature demagnetization (LTD), rocks containing magnetite are cooled to 77 K and rewarmed to room temperature in zero field

* Corresponding author. Tel.: +1 (905) 828 3829; Fax: +1 (905) 828 3717; E-mail: ozdemir@physics.utoronto.ca

0012-821X/99/$ – see front matter
PII: S0012-821X(98)00269-6

in order to erase less stable and reliable components of remanent magnetization. It is unclear whether all the loss of remanence is due to the vanishing of K_1 at T_i or whether the change in crystallographic structure at T_v, accompanied by switching of magnetic easy axes, also plays a role, perhaps even a controlling role. In the present study, by using a carefully oriented crystal of magnetite, we have been able to clearly separate the effects occurring at the two transitions.

The inverse technique to LTD is often used for identifying magnetite in sediments and soils. It consists of producing a synthetic remanence (usually a saturation isothermal remanent magnetization or SIRM) at very low temperature and continuously monitoring the remanence in a zero-field warming–recooling cycle to 300 K. A sudden loss of remanence in warming through T_v, sometimes with a partial recovery on recooling, is diagnostic of magnetite. There is usually little if any remanence change around T_i in this case.

LTD is of considerable interest as a laboratory cleaning technique in paleomagnetism [1–3]. It serves to remove a large part of the remanence due to loosely pinned domain walls in multidomain (MD) grains, thereby isolating the stable remanence [4]. LTD experiments on synthetic magnetites [5,6], crushed natural magnetites [7], natural single crystals [2,8], and magnetite-bearing rocks [9] have shown that the surviving remanence (or magnetic memory) after LTD has single-domain (SD) like properties with high coercivities. As would be expected, memory ratios of both SIRM and thermoremanent magnetization (TRM) increase as the grain size decreases [6]. Crystal defects that strongly pin domain walls also increase the memory and its stability. A comprehensive review appears in Ref. [10].

Recent work has shown that even a large (3 mm) single crystal of magnetite contains distinct SD-like and MD remanence components [11]. The magnetic memory following LTD has the following properties: (1) the memories of SIRM and TRM have SD-like alternating field (AF) decay curves; (2) the SIRM and TRM memories have practically no unblocking temperatures below 560ºC; (3) the memory fraction of high-temperature partial TRM also has mainly blocking temperatures above 565ºC, very similar to those of the total TRM memory. Crystal defects and resulting stress centres, rather than separate SD regions in the crystal, seem to be responsible for the stable SD-like memory.

In many of the LTD experiments described above, measurements were made only at room temperature, before and after cycling the sample to 77 K. In this approach, the data between 300 K and 77 K are lost, including the vitally important properties at the isotropic point and the Verwey transition. In the present study, we therefore continuously monitored the remanent and induced magnetizations of a well-characterized single crystal of magnetite as a function of temperature in both cooling–warming and warming–cooling cycles between 300 K and 10 K. Our purposes were: (1) to clearly separate the isotropic and Verwey transitions and better define their temperatures, T_i and T_v; (2) to understand the effects of crossing T_i and T_v on both room-temperature and low-temperature remanence; (3) to document how the remanences of the high-temperature (cubic) and low-temperature (monoclinic) phases of magnetite change with temperature after crossing the transitions; and (4) to understand the origin of the SD-like magnetic memory of cubic magnetite at room temperature after an LTD cooling–heating cycle.

Our experiments were carried out on a pure, stoichiometric natural single crystal of magnetite, carefully oriented so that the magnetic field was applied along crystallographic principal axes. The crystal quality and purity significantly affect the crystallographic phase transition. Slight deviations from stoichiometry [12] and the presence of cation impurities [13,14] cause broadening and eventual suppression of the Verwey transition. The remanence and other magnetic properties of magnetite also depend strongly on crystallographic orientation. Upon cooling through T_v, the structure changes from cubic spinel to monoclinic. At the same time, the easy directions of magnetization change from <111> to one of the <001> axes.

2. Characterization of the crystal and experimental procedure

Magnetic measurements were carried out on a museum-quality 1.5 mm octahedral crystal of mag-

netite. The {111} crystal faces were flat and smooth, with no striations indicative of deformational twinning. X-ray diffraction using a Debye–Scherrer camera with Cu-Kα radiation and a silicon standard was carried out on a small chip of the crystal. The spinel unit cell edge was 8.402 ± 0.002 Å, in good agreement with the standard value 8.396 Å for magnetite.

The composition of the crystal was determined using a Cameco SX-50 electron microprobe. Chips of the crystal were probed for Fe, O, and seven other elements. Six 10-second counts were recorded for each element at each point and metal standards were referred to before and after each analysis. Each element was measured at six different locations. The analyses gave 72.36 ± 0.23 weight % Fe, close to the theoretical 73.6%. Oxygen concentration was 27.5 ± 0.008 weight %. The weight percents of the other elements were very small: Ti, 0.014 ± 0.003; Mg, 0.002 ± 0.002; Al, 0.081 ± 0.008; Mn, 0.026 ± 0.004; Cr, 0.009 ± 0.003; Ni, 0.005 ± 0.004; and Co, 0.002 ± 0.003. The crystal is stoichiometric magnetite with no major impurities.

The Curie temperature, $T_c = 575$ºC, was determined from the temperature dependence of weak-field susceptibility measured by a Kappa bridge. A continuous jet of argon inhibited chemical alteration during heating.

Induced magnetization M, saturation magnetization M_s, and saturation isothermal remanent magnetization (SIRM) M_{rs} were measured at low temperature using a Quantum Design MPMS2 magnetometer with a SQUID detector. Below the Verwey transition (around $T_v = 120$ K), magnetite is monoclinic, its a, b and c axes corresponding to the $[1\bar{1}0]$, [110] and [001] directions of cubic magnetite above T_v [15]. Our crystal was oriented successively along these three principal axes for measurements. The c axis is the direction of easiest magnetization below T_v; a and b are hard and intermediate directions. The monoclinic c axis may develop in any of the three equivalent <001> axes. A pre-determined c axis was obtained by cooling through T_v in a field of 2.5 T applied along [001].

After the low-temperature experiments were completed, room-temperature hysteresis was measured with a Micro VSM. The room-temperature value of M_s was 93.6 A m^2/kg, as for pure magnetite. The coercive force H_c was 0.11 mT. The ratios M_{rs}/M_s and H_{cr}/H_c (H_{cr} is remanent coercive force) were 0.002 and 47, respectively. These values, together with the ramp-like form of the hysteresis curve, are diagnostic of multidomain grains containing a large number of domain walls.

3. Experimental results

3.1. Induced magnetization curves along principal axes

Fig. 1 shows induced magnetization M as a function of applied field H measured at 10 K along the a, b, and c principal axes. The three magnetization curves have quite different approaches to saturation. Saturation was achieved in relatively low fields of ≈0.2 T in the [001] easy direction but required much higher fields in the $[1\bar{1}0]$ and [110] directions perpendicular to the c axis. Thus the crystal below T_v has essentially uniaxial symmetry. The magnetization curves along the three principal axes can be explained in terms of large magnetocrystalline anisotropy constants. From torque curves measured at 4.2 K, Abe et al. [16] calculated the anisotropy constants of monoclinic magnetite to be $K_a = 25.5 \times 10^4$ J/m^3, $K_b = 3.7 \times 10^4$ J/m^3, and $K_u = 2.1 \times 10^4$ J/m^3.

3.2. Temperature dependence of saturation magnetization M_s

The temperature dependences $M_s(T)$ measured parallel to [001], $[1\bar{1}0]$, and [110] during cooling from 300 K to 10 K in $H = 2$ T are shown in Figs. 2 and 3. In all three crystallographic orientations, M_s increases with decreasing T according to a $(T_c - T)^{0.4}$ relation between 300 K and $T_v = 119$ K. The nearly identical curves show that cubic magnetite is magnetically isotropic in fields ≥2 T above the Verwey transition.

Below T_v, the $M_s(T)$ curves are different for different crystallographic directions. In cooling through the Verwey transition, M_s abruptly decreases by 1.6% and 1.2% for fields applied along $[1\bar{1}0]$ and [110], respectively. The field of 2 T applied during cooling was not enough to saturate the magnetization along these axes below T_v, as seen earlier in

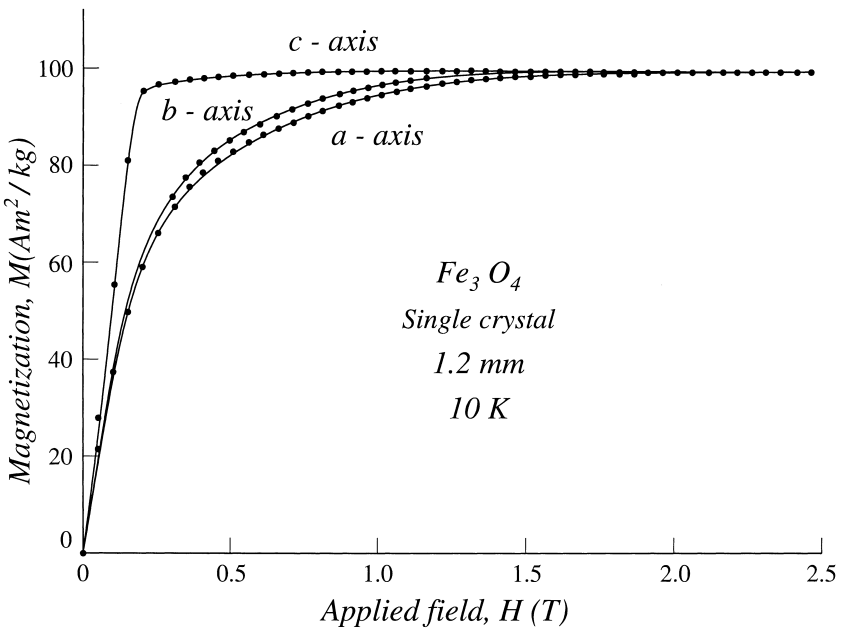

Fig. 1. Induced magnetization M for magnetic field H applied along [1$\bar{1}$0] (monoclinic a axis), [110] (b axis), and [001] (c axis) directions of the magnetite crystal at 10 K.

Fig. 1. These results clearly show that the magnetocrystalline anisotropy of monoclinic magnetite below T_v is much greater than the anisotropy of cubic magnetite above T_v.

Along [001], the 2 T field is very nearly sufficient to saturate the magnetization of the monoclinic phase, and the $M_s(T)$ curve has only a tiny discontinuity of ≈0.1% at the Verwey transition. However, the slope dM_s/dT changes, being lower below T_v. Similar decreases in M_s at the Verwey transition were reported by Uemura and Iida [17] and Matsui et al. [18]. Our measured value of M_s at 10 K is 98.65 A m^2/kg or 4.09 μ_B per formula unit, in good agreement with the theoretical value of 4.0 μ_B per formula unit at 0 K [19].

3.3. SIRM cooling and rewarming: oriented crystal

The crystal was given an SIRM parallel to [001] in a field of 2.5 T at room temperature, then cooled to 10 K and back to 300 K in zero field (Fig. 4). The remanence decreased steadily with cooling to the isotropic temperature, $T_i = 130$ K, where the first magnetocrystalline anisotropy constant K_1 becomes zero. At T_i, 86% of the initial SIRM had been demagnetized. Between T_i and the Verwey transition at $T_v = 119$ K, there was no further demagnetization: the residual 14% of the original SIRM remained constant.

These observations indicate a sharp separation between the two remanence transitions, at T_i and T_v, which has not been clear in previously published data on unoriented crystals. In cooling to T_i, the magnetocrystalline anisotropy decreases to nearly zero; loosely pinned domain walls move as a result, causing a large loss of remanence. Then at $T_v = 119$ K, there is a crystallographic phase transition in which magnetite transforms from cubic to monoclinic. An abrupt increase in the remanence in cooling through T_v (Fig. 4) indicates that [001], the monoclinic c axis, has suddenly become an easy direction of magnetization. In crossing the Verwey transition, the remanence increased more than an order of magnitude, from 0.005 to 0.081 A m^2/kg, which is about 35% higher than the initial SIRM at 300 K.

In further cooling below T_v, the remanence decreased about 10% until 70 K, then remained essentially constant between 70 K and 10 K. The

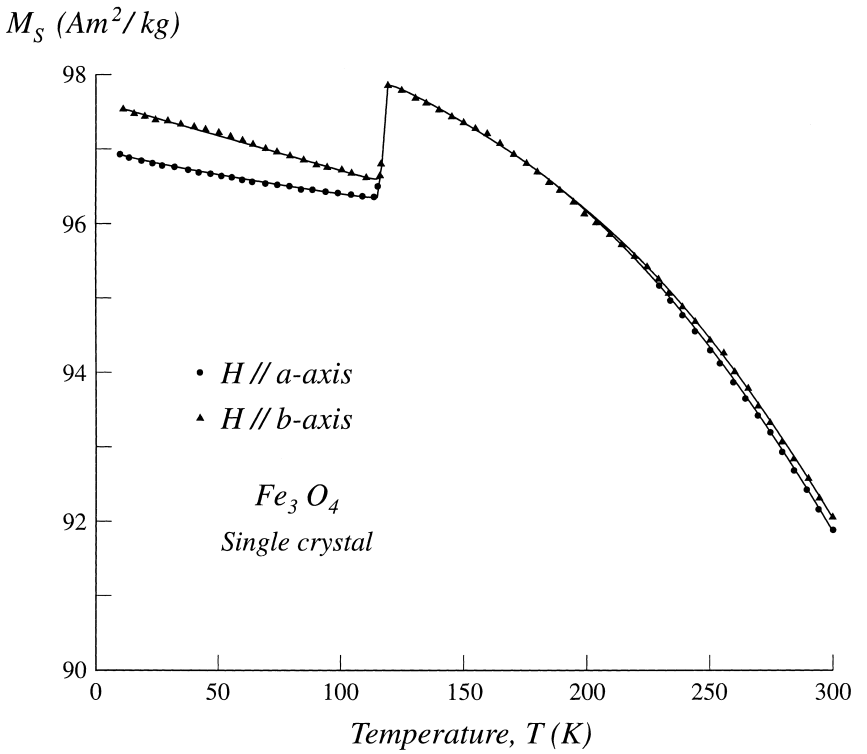

Fig. 2. Temperature dependence of saturation magnetization M_s parallel to [1$\bar{1}$0] and [110] (*a* and *b* axes, respectively) during cooling from 300 K to 10 K in a field $H = 2$ T. The discontinuous drop at the Verwey transition temperature, $T_v = 119$ K, is evidence of the high *a*- and *b*-axis anisotropy of the low-temperature monoclinic phase of magnetite.

remanence at 10 K was 0.0695 A m^2/kg, still an order of magnitude higher than the remanence at T_i or just above T_v.

As the crystal was warmed from 10 K, the remanence retraced the cooling curve, peaking just below T_v and then decreasing dramatically to 0.007 A m^2/kg in crossing the Verwey transition. Thus the process or processes affecting the remanence of the monoclinic magnetite below T_v are perfectly reversible. No permanent demagnetization is involved. Furthermore, the remanence recovered by the cubic magnetite above T_v is virtually identical to the remanence before cooling through T_v and remains constant in heating to 300 K. There is no recovery of remanence at or above T_i. It is clear that all irreversible change in the remanence occurred during zero-field cooling to T_i. The ultimate SIRM memory at 300 K is completely unaffected by the large, but reversible, changes in the cooling–heating cycle below T_i. Thus low-temperature demagnetization is governed entirely by the vanishing of magnetocrystalline anisotropy at the isotropic temperature and are unaffected by changes in crystallographic structure at the Verwey transition. Although the two transitions are only about 10 K apart, they are distinct and have quite different effects on remanence.

3.4. SIRM cooling and rewarming: unoriented crystal

A new SIRM was produced by applying a 2.5 T field at room temperature with the crystal unoriented. The subsequent zero-field cooling and reheating curves are illustrated in Fig. 5. In cooling from 300 K to T_v, the remanence of the unoriented crystal decreased in the same way as that of the oriented crystal (Fig. 4). However, the unoriented crystal had a 20% higher SIRM intensity. This difference arises because in the oriented crystal, the field was applied along [001], a hard direction of magnetization

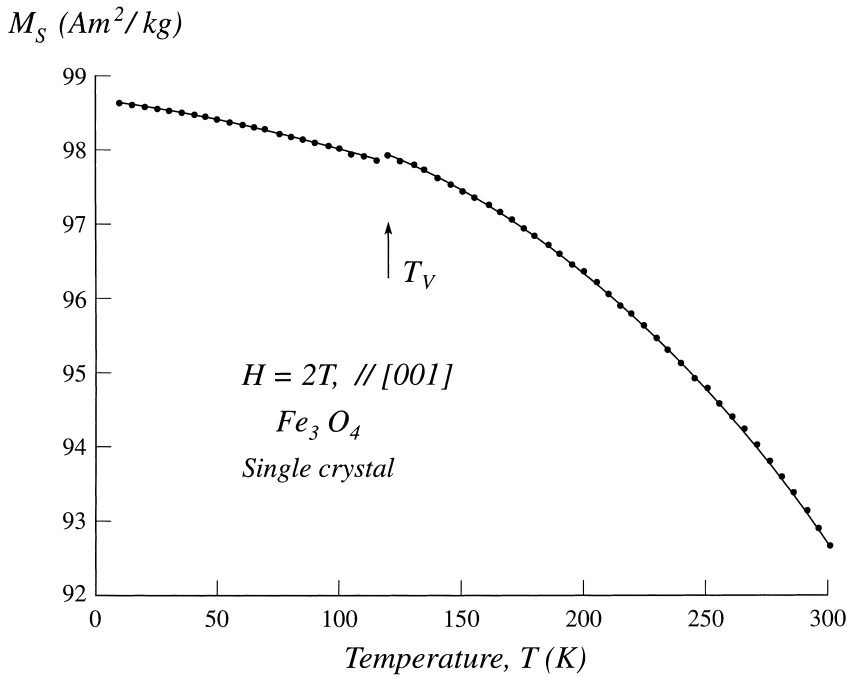

Fig. 3. M_s–T curve along the cubic [001] direction (monoclinic c axis) of the crystal during cooling from 300 K to 10 K in a field H = 2 T. There is hardly any discontinuity in M_s in crossing the Verwey transition because the anisotropy is much less along the c axis than along the a or b axes below T_v.

for cubic magnetite. In a randomly oriented crystal, <111> easy axes are closer to the field direction and consequently the SIRM is larger.

By 119 K, 89% of the initial SIRM had been destroyed. This soft fraction, carried by weakly pinned domain walls, is almost the same as in the oriented crystal (Fig. 4). However, the isotropic point is not as clearly separated from the Verwey transition as it was for the oriented crystal.

Cooling below T_v resulted in a sudden increase in remanence (119–110 K), followed by a smaller, more gradual decrease (110–100 K). Both changes were repeated exactly in heating from 10 K. Although the cooling and reheating curves below T_v are similar in shape to those of the oriented crystal, the remanence increase across the Verwey transition is a factor 6 smaller and is spread over a wider temperature interval. The very large, step-like remanence increase in the oriented crystal occurs because [001] becomes an easy axis below T_v and the entire remanence is oriented in this direction. In the unoriented crystal, the domains reorient themselves along three orthogonal <001> axes, each with only a small component of magnetization in the measurement direction.

In reheating above T_v, the remanence does not retrace the cooling curve but is almost temperature independent. The heating and cooling curves do not match between T_v and T_i as they did for the oriented crystal. The SIRM memory at room temperature is about 11%. Similar SIRM cooling and warming curves with some remanence rebound across the transition have been observed for other unoriented single crystals of magnetite [4].

3.5. SIRM warming curve for the oriented crystal

The oriented crystal was given a new SIRM at 20 K by applying a 2.5 T field along the monoclinic c-axis, i.e., the cubic [001] direction. It was then warmed in zero field to 300 K (Fig. 6). The behaviour was much simpler than in cooling of room-temperature SIRM. The remanence was almost constant between 20 K and 100 K. Just below and at T_v,

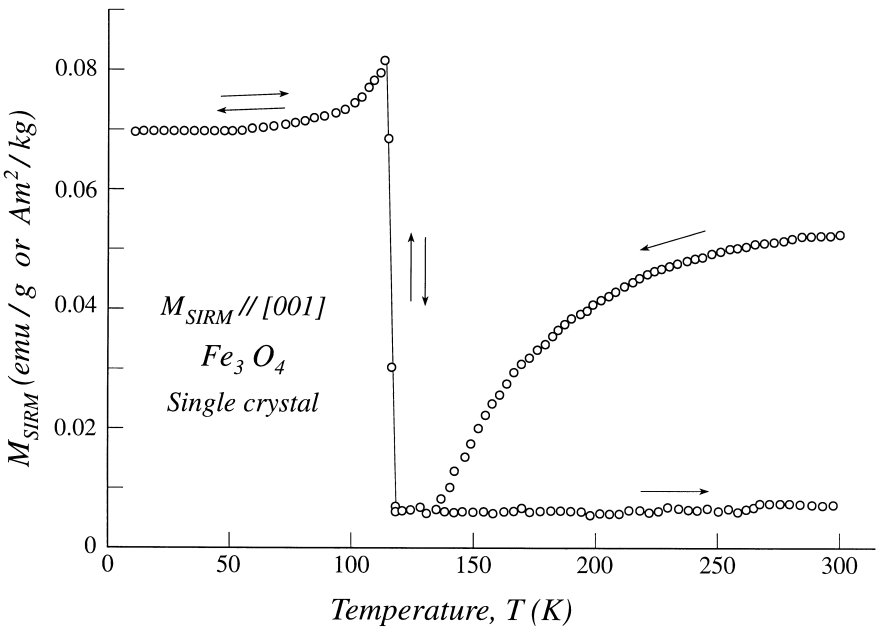

Fig. 4. Temperature dependence of saturation remanence (SIRM) M_{SIRM}, produced by a 2.5 T field along [001] at 300 K, during zero-field cooling from 300 K to 10 K and zero field warming back to 300 K. The magnetic isotropic point at $T_i = 130$ K and the Verwey transition at $T_v = 119$ K are cleanly separated in the data. All irreversible loss of remanence occurs between 300 K and T_i; there is no further change between T_i and T_v. There is a large but reversible jump in remanence intensity at T_v when the cubic [001] hard direction becomes the monoclinic c axis, the direction of easy magnetization. Notice that the SIRM cooling and heating curves are irreversible for the high-temperature cubic phase but completely reversible at all temperatures below T_v for the monoclinic phase.

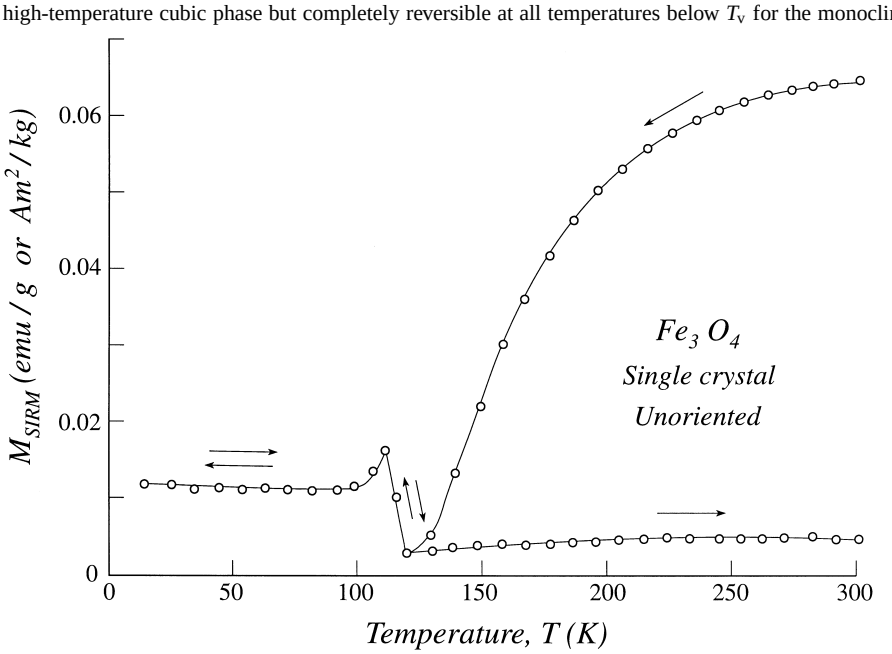

Fig. 5. The zero-field cooling and warming curves of SIRM for the same magnetite crystal when it is magnetized and its remanence measured in an arbitrary orientation with respect to the principal crystallographic axes. The effects of T_i and T_v on the remanence cannot be clearly separated for the unoriented crystal.

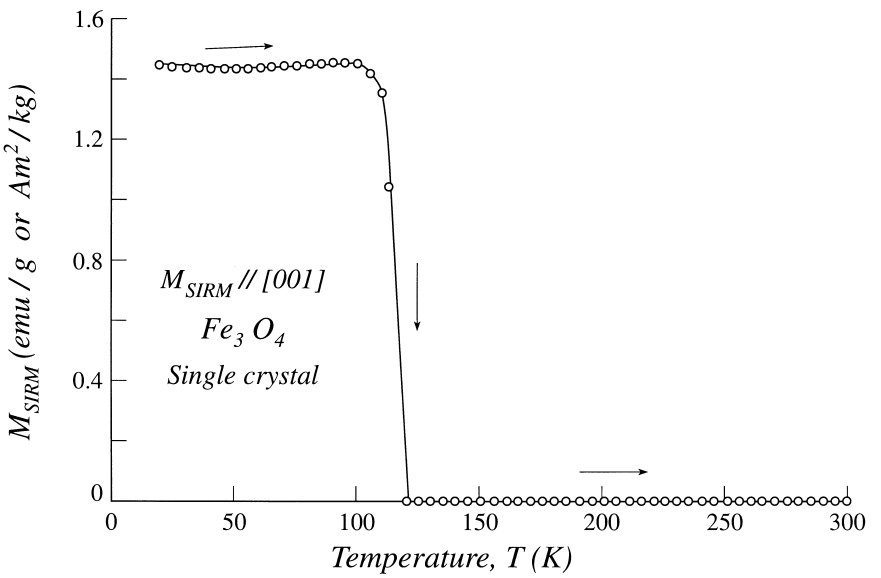

Fig. 6. Zero-field SIRM warming curve from 20 K to 300 K for the same magnetite crystal. SIRM was produced in a field of 2.5 T at 20 K along the monoclinic *c* axis (cubic [001]). The behaviour is simple in this case: the remanence, which is about 30 times stronger than the room-temperature SIRM in Fig. 4, is constant below T_v then decreases to zero in crossing the Verwey transition.

the remanence decreased essentially to zero, where it remained in warming to 300 K. Thus SIRM produced at low temperature in monoclinic magnetite is completely demagnetized in the transition to the cubic phase and no memory of the original SIRM is recovered in recooling through T_v, in our crystal at least. This behaviour is entirely different from that of room-temperature SIRM cycled to low temperature and back to 300 K (Fig. 4).

The sharp decrease in remanence at T_v in the SIRM warming curve is diagnostic of stoichiometric magnetite and has been observed previously for reduced submicron magnetites [12]. Our measured value of 119 K for T_v agrees well with previous determinations for stoichiometric magnetite crystals [20–22]. A striking result in Fig. 6 is the high intensity of low-temperature SIRM: 1.45 A m^2/kg, about 30 times higher than room-temperature SIRM. Part of the difference is due to the fact that [001] is the monoclinic easy axis but a cubic hard axis. However, to explain such a large contrast, there must be quite different domain configurations in the SIRM state at 20 K and 300 K. The high uniaxial anisotropy of the low-temperature monoclinic phase must pin domain walls much farther from their equilibrium positions.

4. Discussion

Cooling our crystal in zero field through the isotropic point at $T_i = 130$ K resulted in the permanent loss of 86% of the room-temperature SIRM (Fig. 4). This decrease in remanence with cooling below 300 K is mainly due to progressive jumps of loosely pinned domain walls [4]. According to Kittel [23], the 180° Bloch wall thickness w is given by

$$w = \pi(A/K_u)^{1/2} \quad (1)$$

where A is the exchange constant and K_u is the effective magnetic anisotropy, which is the sum of the magnetocrystalline and magnetoelastic anisotropies [24]:

$$K_u = -(2/3)K_1 + (9/2)c_{44}\lambda_{111}^2 \quad (2)$$

Since K_1, λ_{111} and c_{44} all decrease with decreasing temperature (apart from a minor increase in K_1 just below room temperature), the wall thickness below room temperature increases with cooling. Broad walls are less effectively pinned by localized defects and eventually escape. At 130 K, K_1 becomes zero and changes sign. Domain walls blocked by magnetocrystalline controlled pinning become free to jump

and lead to demagnetization of a large fraction of remanence. These loosely pinned walls are also easily moved by alternating fields or heating. Özdemir and Dunlop [11] found that the fraction of remanence erased by LTD in a large crystal of magnetite had low coercivities and a broad spectrum of low unblocking temperatures.

The remaining 14% of the room-temperature SIRM was not destroyed by cycling through T_i. Even cycling through T_v had no effect on this SIRM memory, which is due to strongly pinned domain walls, probably pinned magnetostrictively by dislocations or other crystal defects. Although K_1 becomes zero and changes sign at the isotropic point, λ_{111}, λ_{100}, and c_{44} are not zero, making an important contribution to the magnetoelastic anisotropy that controls the magnetic memory. These walls are so strongly pinned by the stress fields of crystal defects that the remanence they carry is independent of temperature during reheating from T_i to 300 K (Fig. 4). This pinning may explain the SD-like memories observed in small and large MD magnetites [2,5,6]. Özdemir and Dunlop [11] found that the memories of TRM, partial TRM, and SIRM of 3-mm and 4.5-mm magnetite crystals had SD-like AF decay curves with initial plateaus of no demagnetization and thermal demagnetization curves with no unblocking temperatures below 560°C.

The hardness of the SD-like remanence was attributed to the strong pinning of walls by defect concentrations at monoclinic twin boundaries [11]. However, Fig. 4 clearly indicates that the cubic → monoclinic transition occurs ≈10 degrees below the isotropic point, and the memory is temperature independent between T_i and T_v. Although monoclinic twinning probably plays an important role in controlling the remanence below the Verwey transition, it has no effect on the memory of cubic magnetite above T_v. On the other hand, if the SIRM is imparted at low temperature and the Verwey transition is approached from below, a major part of the remanence is lost at T_v and there is no indication of any further change at T_i (Fig. 6). Most of the decrease at T_v is permanent, with almost no recovery in the second crossing of the Verwey transition in the cooling half of the cycle.

The room-temperature SIRM behaves in a completely different way as the Verwey transition is approached from above, crossed, and then recrossed in the warming half of the cycle. Although there is again a sudden large change in remanence at T_v in the first crossing (in this case an increase), the effect is completely reversible (Figs. 4 and 5). In recrossing the transition, the remanence reverts to its original level.

The discontinuous change in remanence is much more pronounced when the crystal is oriented so that SIRM is produced and measured along [001], which becomes the *c* axis of the monoclinic phase below T_v. One reason for this is the following. Since [001] is a hard axis above T_v, the domains that carry the SIRM have a choice of four equivalent <111> easy directions, which make identical angles of 54.7° with [001] and are arranged symmetrically about [001]. These domain magnetizations are to a considerable extent mutually cancelling, leading to a relatively small SIRM. However, in crossing T_v, [001] becomes the monoclinic easy axis and all the domain magnetizations rotate into this direction. The remanence increases accordingly. In recrossing the transition, the domain magnetizations revert to the initial set of equally spaced <111> directions and the remanence drops back to its original level.

When the crystal is not oriented along [001], one of the <111> directions is necessarily closer to the field direction than the others and is preferred by the domain magnetizations. The SIRM will be larger, as we observe, but the change across the Verwey transition will be less (Fig. 5), for two reasons. First, the remanence below T_v cannot be as large as in the crystal oriented along the monoclinic easy axis. Second, it is not certain that only one of the set of <001> axes is chosen as the *c*-axis throughout the unoriented crystal, so that the domains may have a choice of competing magnetization directions below T_v. Indeed monoclinic twinning is well established in magnetite. In assemblages of randomly oriented MD crystals, for example glass–ceramic magnetites [4], so many competing directions are available that no increase is observed across the transition.

This general explanation assumes that domain walls remain pinned in the same positions in crossing the Verwey transition, with only the directions of the domain magnetizations changing. However, this model can only account for a remanence increase of $1/\cos 54.7^\circ = 1.73$ at most, and the in-

crease in Fig. 4 is much larger than this. Therefore the discontinuous change in remanence is probably controlled in part by discontinuous changes in magnetic anisotropy, magnetostriction, and magnetoelastic constants due to the switching of the easy axes at T_v. The magnetic anisotropy constants of the low-temperature phase of magnetite are expressed in terms of K_a, K_b, K_u, K_{aa}, K_{bb}, and K_{ab} [25]. They are all positive and temperature dependent. Abe et al. [16] calculated the thermal variation of K_1 values and showed that the K_1(T) curve has a discontinuous increase at the Verwey transition. The temperature variations of the magnetostriction constants λ_{111}, λ_{100} and λ_s also show abrupt changes at the phase transition [22]. Moran and Lutfi [26] measured the temperature dependence of c_{44}, which likewise exhibits a discontinuous increase at the phase transition. According to Eqs. 1 and 2, any increases in magnetocrystalline, magnetostriction, and magnetoelastic constants at T_v will result in a decrease in the domain wall thickness. Then the domain walls will be very efficiently pinned by internal stresses due to crystal defects. This does not of itself explain the observations in Fig. 4, however, because walls must move in order to accomplish a further increase in remanence.

Another factor controlling the remanence below T_v is the presence of monoclinic twin boundaries (TWB). As the crystal cools through T_v, it acquires a twin structure [16,18,20,27]. Electron microscope observations at 77 K show two kinds of TWB's between monoclinic twins with orthogonal *c* axes. One type of TWB is perpendicular to one of the *c* axes, and the other makes a 45° angle with both *c* axes [27]. Twinning of the monoclinic crystal with respect to the orientation of the *a* and *b* axes introduces strain at the TWB's [28]. The twin junctions become regions of maximum strain which can act as pinning centres for domain walls. Wall pinning at the TWB's must be strong enough to bring the remanence to a peak value of 0.08 A m^2/kg, which is an order of magnitude higher than the value just above T_v. As the crystal is warmed, the process is reversed. At T_v, the monoclinic TWB's will disappear, resulting in domain wall unpinning and a sudden decrease in remanence. In Fig. 4, the cooling and warming curves coincide within the accuracy of the drawing. This is consistent with the reversible appearance of TWB's upon cooling across T_v and their disappearance on subsequent heating.

5. Conclusions

SIRM cooling/rewarming curves provide important information about low-temperature demagnetization (LTD). LTD destroys remanence due to the loosely pinned domain walls (magnetocrystalline pinning), leaving strongly pinned walls (magnetoelastic pinning) and possibly other sources of remanence as the carriers of low-temperature memory. All unpinning occurs at T_i in our crystal.

There is a clean separation between the two remanence transitions in our magnetite crystal. The magnetic isotropic point, where the first magnetocrystalline anisotropy constant passes through zero, is at $T_i = 130$ K. The Verwey transition, at which the crystal structure changes from cubic to monoclinic, occurs at $T_v = 119$ K.

The shapes of the remanence curves and other magnetic properties at temperatures below and above the Verwey transition depend strongly on the crystallographic orientation of the crystal.

When the crystal is cooled below the Verwey transition, the crystal is more difficult to magnetize to saturation along the *a* and *b* axes, which are the hard and medium directions of magnetization. The crystal is much easier to magnetize along the *c*-axis (cubic [001] direction). These observations (Fig. 1) indicate that the magnetic symmetry has been reduced from cubic to uniaxial at T_v.

Monoclinic twin formation just below the Verwey transition has a significant effect on the hardness and intensity of SIRM. The twin boundaries interact strongly with the domain walls and tend to act as wall pinning sites.

Room-temperature and low-temperature SIRM's behave entirely differently in thermal cycles across the Verwey transition. Low-temperature SIRM drops irreversibly to almost zero in heating across T_v, with very little recovery in the second crossing. High-temperature SIRM increases sharply in cooling across T_v, but the behaviour at and below T_v is completely reversible and the original remanence level is recovered in the second crossing. Warming a low-temperature SIRM pinpoints the Verwey transition

and is a good method of identifying magnetite, but it gives no information about remanence changes near the isotropic point T_i.

Acknowledgements

We thank Malcolm Back of the Royal Ontario Museum, Toronto for donating the natural single crystal of magnetite and Sue Halgedahl and Ron Merrill for helpful reviews. These measurements were carried out at the Institute for Rock Magnetism at the University of Minnesota, which is operated with funding from the National Science Foundation and the Keck Foundation. We are grateful to Drs. Subir Banerjee and Bruce Moskowitz for welcoming us Visiting Fellows and to Jim Marvin and Mike Jackson for help with the instruments. ***[RV]***

References

[1] M. Ozima, M. Ozima, T. Nagata, Low temperature treatment as an effective means of 'magnetic cleaning' of natural remanent magnetization, J. Geomagn. Geoelectr. 16 (1964) 165–177.

[2] K. Kobayashi, M. Fuller, Stable remanence and memory of multidomain materials with special reference to magnetite, Philos. Mag. 18 (1968) 601–624.

[3] R.T. Merrill, Low-temperature treatments of magnetite and magnetite-bearing rocks, J. Geophys. Res. 75 (1970) 3343–3349.

[4] S.L. Halgedahl, R.D. Jarrard, Low-temperature behavior of single-domain through multidomain magnetite, Earth Planet. Sci. Lett. 130 (1995) 127–139.

[5] D.J. Dunlop, K.S. Argyle, Separating multidomain and single-domain-like remanences in pseudo-single-domain magnetites (215–540 nm) by low-temperature demagnetization, J. Geophys. Res. 96 (1991) 2007–2017.

[6] F. Heider, D.J. Dunlop, H.C. Soffel, Low-temperature and alternating field demagnetization of saturation remanence and thermoremanence in magnetite grains (0.037 μm to 5 mm), J. Geophys. Res. 97 (1992) 9371–9381.

[7] E. McClelland, V.P. Shcherbakov, Metastability of domain state in multidomain magnetite: consequences for remanence acquisition, J. Geophys. Res. 100 (1995) 3841–3857.

[8] M. Ozima, M. Ozima, S. Akimoto, Low-temperature characteristics of remanent magnetization of magnetite −− self reversal and recovery phenomena of remanent magnetization, J. Geophys. Res. 16 (1964) 165–177.

[9] J.P. Hodych, R.I. Mackay, G.M. English, Low-temperature demagnetization of saturation remanence in magnetite-bearing dolerites of high coercivity, Geophys. J. Int. 132 (1998) 401–411.

[10] D.J. Dunlop, Ö. Özdemir, Rock Magnetism: Fundamentals and Frontiers, Cambridge University Press, New York, 1997, 573 pp.

[11] Ö. Özdemir, D.J. Dunlop, Single-domain-like behavior in a 3-mm natural single crystal of magnetite, J. Geophys. Res. 103 (1998) 2549–2562.

[12] Ö. Özdemir, D.J. Dunlop, B.M. Moskowitz, The effect of oxidation on the Verwey transition in magnetite, Geophys. Res. Lett. 20 (1993) 1671–1674.

[13] Z. Kakol, A. Kozlowski, J. Sabol, P. Metcalf, J.M. Honig, Cation distribution in $Fe_{3(1-\delta)}O_4$ and low level doped $Fe_{3-x}M_xO_4$, M = Ti, Zn, Al, Acta Phys. Pol. 85 (1994) 223–227.

[14] A. Kozlowski, Z. Kakol, R. Zalecki, J.M. Honig, Specific heat of low doped magnetite, $Fe_{3-x}Ti_xO_4$ and $Fe_{3-y}Zn_yO_4$, J. Magn. Magn. Mat. 144 (1995) 2083–2084.

[15] S. Iida, Structure of Fe_3O_4 at low temperatures, Philos. Mag. 42 (1980) 349–376.

[16] K. Abe, Y. Miyamoto, S. Chikazumi, Magnetocrystalline anisotropy of low temperature phase of magnetite, J. Phys. Soc. Jpn. 41 (1977) 1894–1902.

[17] S. Uemura, S. Iida, Accurate measurement of magnetization of Fe_3O_4 in the vicinity of the transition, J. Phys. Soc. Jpn. 40 (1976) 679–685.

[18] M. Matsui, S. Todo, S. Chikazumi, Magnetization of low temperature phase of Fe_3O_4, J. Phys. Soc. Jpn. 43 (1977) 47–52.

[19] J. Smit, H.P.J. Wijn, Ferrites, Wiley, New York, 1959, 369 pp.

[20] B.A. Calhoun, Magnetic and electric properties of magnetite at low temperatures, Phys. Rev. 94 (1954) 1577–1585.

[21] K.I. Arai, K. Ohmori, N. Tsuya, S. Iida, Magnetostriction of magnetite in the vicinity of the low-temperature transition, Phys. Stat. Sol. 34 (1976) 325–330.

[22] N. Tsuya, K.I. Arai, K. Ohmuri, Effect of magnetoelastic coupling on the anisotropy of magnetite below the transition temperature, Physica B 88 (1977) 959–960.

[23] C. Kittel, Physical theory of ferromagnetic domains, Rev. Mod. Phys. 21 (1949) 541–583.

[24] S. Xu, R.T. Merrill, Thermal variation of domain wall thickness and number of domains in magnetic rectangular grains, J. Geophys. Res. 95 (1990) 21433–21440.

[25] W. Palmer, Magnetocrystalline anisotropy of magnetite at low temperature, Phys. Rev. 131 (1963) 1057–1062.

[26] T.J. Moran, B. Lűthi, Elastic and magnetoelastic effects in magnetite, Phys. Rev. 187 (1969) 710–714.

[27] S. Chikazumi, K. Chiba, K. Suzuki, T. Yamada, Electron microscopic observation of low temperature phase of magnetite, in: Y. Hoshino, S. Iida, M. Sugimoto (Eds.), Ferrites: Proceedings of the International Conference, Univ. of Tokyo Press, Tokyo, 1971, pp. 141–143.

[28] A. Putnis, Introduction to Mineral Sciences, Cambridge University Press, New York, 1995.